The Cryosphere Discuss., 7, 2891–2941, 2013
www.the-cryosphere-discuss.net/7/2891/2013/
doi:10.5194/tcd-7-2891-2013

The Cryosphere Discussions
Open Access

2001–2010 glacier changes in the Central Karakoram National Park: a contribution to evaluate the magnitude and rate of the "Karakoram anomaly"

U. Minora[1,3], D. Bocchiola[1,2], C. D'Agata[1,3], D. Maragno[1,3], C. Mayer[1,4], A. Lambrecht[1,4], B. Mosconi[3], E. Vuillermoz[1], A. Senese[3], C. Compostella[3], C. Smiraglia[1,3], and G. Diolaiuti[1,3]

[1]Evk2cnr Committee, Bergamo, Italy
[2]Politecnico di Milano, Milan, Italy
[3]Università degli Studi di Milano, Milan, Italy
[4]Bavarian Academy of Sciences and Humanities, Munich, Germany

Received: 7 May 2013 – Accepted: 21 May 2013 – Published: 18 June 2013

Correspondence to: G. Diolaiuti (guglielmina.diolaiuti@unimi.it)

Published by Copernicus Publications on behalf of the European Geosciences Union.

Abstract

Karakoram is one of the most glacierized region worldwide, and glaciers therein are the main water resource of Pakistan. The attention paid to this area is increasing, because the evolution of its glaciers recently depicted a situation of general stability, known as "Karakoram Anomaly", in contrast to glacier retreat worldwide. Here we focused our attention upon the glacier evolution within the Central Karakoram National Park (CKNP, a newborn park of this region, ca. 12 162 km^2 in area) to assess the magnitude and rate of such anomaly. By means of Remote Sensing data (i.e.: Landsat images), we analyzed a sample of more than 700 glaciers, and we found out their area change between 2001 and 2010 is not significant (+27 km^2 ± 42 km^2), thus confirming their stationarity. We analyzed climate data, snow coverage from MODIS, and supraglacial debris presence, as well as potential (con-) causes. We found a slight decrease of summer temperatures (down to −1.5 °C during 1980–2009) and an increase of wet days during winter (up +3.3 days yr^{-1} during 1980–2009), possibly increasing snow cover duration, consistently with MODIS data. We further detected considerable supraglacial debris coverage (ca. 20 % of the glacier area which rose up to 31 % considering only the ablation area), which could have reduced buried ice melting during the last decade. These results provide further ground to uphold the existence of the Karakoram Anomaly, and present an useful template for assessment of water availability within the glaciers of the CKNP.

1 Introduction

The HKKH (Hindu Kush–Karakoram–Himalaya) stretches for more than 2000 kilometres in length from East to West. Along this mountain range there is a considerable variability in climate conditions, including varying source regions and type of precipitation (e.g. Bocchiola and Diolaiuti, 2013), influencing the behaviour and evolution of cryosphere. The HKKH nests about 60 000 km^2 of ice bodies, glaciers, glacierets and

perennial surface ice in varying climatic regimes (Kääb et al., 2012), and it is considered the third pole of our planet (Winiger et al., 2005; Smiraglia et al., 2007; Kehrwald et al., 2008). This large mountain system delivers water for agriculture, human consumption and power production, and more than 50 % of the water in the Indus river originating from the Karakoram comes from snow and glacier melt (Immerzeel et al., 2010). The economy of the Himalayan regions relies upon agriculture, and it is highly dependent upon water availability and irrigation (Aggarwal et al., 2004; Kahlown et al., 2007; Akhtar et al., 2008). The most recent observations of glacier fluctuations indicate that in the eastern and central HKKH glaciers are subject to general retreat, and have lost a significant amount of mass and area (Salerno et al., 2008; Bolch et al., 2011). Rapid declines in glacier area is reported throughout the Greater Himalaya and most of mainland Asia (Ageta, and Higuchi, 1984; Ageta, and Fujita, 1996), widely attributed to global warming (IPCC, 2001, 2007). On the other hand changes in climate and glaciers geometry are not uniform. Observations of individual glaciers indicate that the glacier retreat rates may vary strongly from among different glacial basins. In fact positive ice mass balances and advancing glaciers have been reported in the Karakoram mountains, since the last decade, in spite of worldwide glacier decline (Hewitt, 2005). Glaciers in the Eastern part of the HKKH receive accumulation from precipitation during the Indian monsoon in summer, whereas in the West snow fall occurs mainly in winter, through Westerly atmospheric circulations (Bookhagen and Burbank, 2010; Kääb et al., 2012; Fowler and Archer, 2006). This variability in accumulation conditions may be one reason for the large spread in glacier changes within the region (Bolch et al., 2011; Kääb et al., 2012). Among others, Kääb et al. (2012) indicated a complex pattern of glacial responses in reaction to heterogeneous climate signals. They used satellite laser altimetry and a global elevation model to show widespread glacier wastage in the Eastern, central and South–Western parts of the HKKH during 2003–08. The maximum regional thinning rate they found was $-0.66 \pm 0.09\,\mathrm{m\,yr^{-1}}$ in the Jammu–Kashmir region. Conversely, in the Karakoram, glaciers seem to have thinned by a few centimetres per year, with this behaviour not linked only to the widespread supra-glacial debris

cover. Unexpectedly, regionally averaged thinning rates under debris-mantled ice were similar to those of clean ice. The glacier mass balance budget in the Karakoram positively affected the 2003–2008 specific mass balance for the entire HKKH region, which was estimated by Kääb et al. (2012) into $-0.21 \pm 0.05\,\mathrm{m\,yr^{-1}}$ of water equivalent. This is significantly smaller in magnitude than the estimated global average for glaciers and ice caps (Cogley 2009; WGMS, 2012). Some studies display not only balanced to slightly negative mass budgets in the Karakoram range, but even an expansion and thickening of the largest glaciers, mainly in the central Karakoram, since the 1990s, accompanied by a non-negligible number of rapid glacier advances (i.e.: surge-type phenomena, see among the others Diolaiuti et al., 2003; Hewitt, 2005; Barrand and Murray, 2006; Belò et al., 2008; Mayer et al., 2011; Copland et al., 2011).

This situation of stagnant and advancing glaciers in the highest parts of central Karakoram was called "Karakoram anomaly" by Hewitt (2005), and more recently the "Pamir–Karakoram Anomaly" name was proposed by Gardelle et al. (2013). Hewitt (2005) reported that 33 glaciers thickened (by 5 to 20 m on the lowest parts of their tongues) and/or advanced, or at least were stagnant in this region between 1997 and 2001. For instance, 4 tributaries of Panmah Glacier have surged in less than a decade, 3 in quick succession. Liligo Glacier, a tributary of Baltoro Glacier, advanced by 1.4 km from 1986 to 1997 (Diolaiuti et al., 2003). Batura and Baltoro had stagnant termini, although accompanied by down wasting and debris cover increase in the lowest reaches (Shroder et al., 2010; Mayer et al., 2006).

In general glaciers in the Karakoram range seem to be less affected by the global trend of negative glacier mass balance, with frequent observations of advancing glaciers. This behaviour might be a consequence of the generally high elevations of glaciers' bodies in this area, combined with a possible increase in orographic precipitation leading to enhanced accumulation. These observations were explained with the recent climate peculiarities, i.e. (i) a decreasing trend in maximum and minimum temperatures in some periods within the Karakoram range, and (ii) an increase in winter precipitation (Archer and Fowler, 2004; Bocchiola and Diolaiuti, 2013). The negative

temperature trend during summer is consistent with observed advance and thickening of some Karakoram glaciers, and the reducing runoff shown by some gauging station data from heavily glacierized catchments (e.g. Hunza basin, Hewitt, 2005; Archer, 2003). An in depth scientific understanding of the glacier evolution of the Karakoram was hampered hitherto by the lack of systematic long-term field observations, due to the rugged topography and the complex climatology of the area. The annual glacier mass balances of a few small and mainly debris-free glaciers (Fujita and Nuimura, 2011; Gardelle et al., 2012) are unlikely to be representative of the entire region with some of the world's largest glaciers. Therefore the combination of remote sensing studies and data from field surveys is required for improving the understanding of glacier dynamics related to the specific climate conditions. In this contribution we present the main results we obtained analysing Landsat images covering the Central Karakoram National Park (CKNP) area to describe glacier coverage during 2001–2010. We further processed meteorological data provided by the Pakistan Meteorological Department (PMD), including precipitation and air temperature during 1980–2009 from three stations in the upper Karakoram nearby the CKNP. These data were also tested against the Northern Atlantic Oscillation (NAO) index and global temperature anomalies (HADCRUT data set, see Brohan et al., 2006) to assess potential teleconnections, claimed recently to affect the climate in this area. We then evaluated snow-coverage in the CKNP area during 2000–2011 from MODIS data, and supraglacial debris-coverage variations during 2001–2010 from Landsat images. From the intercomparison of the different data sources exploited here we try to draw an updated picture of the CKNP glaciation, and discuss its peculiar behavior and features against the recent literature upon HKKH glacier changes.

2 Study site

The CKNP is an extensive, newborn protected natural area within the Karakoram, Northern Pakistan (Fig. 1). The park area is ca. 12 162 km^2, and roughly 40 % of it

is covered by ice. The park's mission is to preserve unimpaired natural and cultural resources of this peculiar area, supporting the study and interpretation of this heavily glacierized environment and its population of birds and mammals. There are some glaciers that intersect the park boundary, and therefore we modified CKNP boundary so as to include all glacier outlines, covering an area of 13 199 km^2, which we considered when calculating glacierized versus not-glacierized area statistics in this paper.

The Park is a new protected area, funded in the last decade. Several scientists from Pakistan and Italy are cooperating to develop a Park Management Plan, implementing best practices of environmental surveys within the framework of the SEED (Social Economic Environment Development in the Central Karakorum National Park, Gilgit Baltistan Region) project, funded by the Pakistan and Italian governments, and managed by EvK2CNR Committee. The highest altitude in the park, and in the entire western HKKH is reached by the summit of K2 mountain (8611 m a.s.l.). According to the Köppen–Geiger climate classification this area is a cold desert region, or BWK region, with a dry climate, little precipitation, and a wide daily temperature range (Peel et al., 2007). The HKKH area displays a considerable altitude range, influencing climatic conditions. The Nanga Parbat massif forms a barrier to the Northward movement of monsoon storms, which intrude little into Karakoram. Thus, the hydrological regime in this region is only partly influenced by the monsoon, while a major contribution results from seasonal snow and glacier melt. Precipitation occurs in two main periods, winter (JFM) and summer (JAS), i.e. driven by the westerly currents and monsoon respectively, and the winter precipitation provides the dominant nourishment for the glacier systems of the HKKH (Bocchiola and Diolaiuti, 2013). Some studies postulate that these mountains gain a total annual rainfall between 200 mm and 500 mm, amounts that are generally derived from valley-based meteorological stations and which are less representative for the highest elevation zones (Archer, 2003). High elevation snowfall is still rather unknown, due to the difficulty of obtaining reliable measurements. Some estimates from snow pits above 5000 m a.s.l. range from 1000 mm to more than 3000 mm yr^{-1}, depending upon site (Winiger et al., 2005; the authors of this study, unpublished data).

However, there is considerable uncertainty about the spatial distribution and the vertical gradient of precipitation at high altitudes. Among the natural elements within the CKNP glaciers probably show the largest temporal variations. Within the park there are more than 700 glaciers, spanning a broad range of size, geometry, type, and surface conditions (i.e. debris free and debris covered ice). The Baltoro glacier, one of the most prominent glaciers in the park, is about 60 km long, and it is one of the largest debris covered glaciers worldwide. Baltoro glacier has been studied for more than one century, within several scientific expeditions, among others those led by Ardito Desio, a most renowned Italian scientist and explorer (Desio, 1954; Mayer et al., 2006). It is not fully clear how results from the temperate zones can be applied to understand the dynamics of glaciers within the monsoon-dominated region of HKKH (Kaser et al., 2003), and also in central Karakoram, with a reduced influence of monsoon precipitation, the climate-glacier relation is not investigated in detail. The glacier-climate-hydrology interactions in the lower latitudes are of great interest for both global and regional purposes, and a network of well-chosen and carefully monitored glaciers is important to establish a base for investigating these relationships (Kaser et al., 2003). In addition, accurate observation of glaciers' coverage and dynamics is needed to understand the role of cryosphere in hydrology and water resources. The SEED project is focusing upon providing these data base, e.g. by developing the CKNP glacier inventory for different periods. This is a base for (i) describing the present characteristics of glaciation in the Park and its features and, (ii) evaluating glacier changes within a time window of about a decade. The main results from this research activity are presented in this paper, including the interpretation of the observed glacier dynamics against climate trends from meteorological data provided by the Pakistan Meteorological Department (PMD), covering the period 1980–2009, and against maps of snow cover area from MODIS satellite during 2001–2011.

3 Methods

3.1 Glacier data

3.1.1 The CKNP glacier inventory

On a global scale, glacier outlines can be derived using automated classification algorithms from multispectral satellite data (e.g. Paul et al., 2004a,b; Paul and Kääb, 2005), as recommended in the the Global Terrestrial Network for Glaciers (GTN-G, Haeberli, 2006).

For the compilation of the CKNP Glacier Inventory we followed the new and updated recommendations suggested by Paul et al. (2010), and we considered the main parameters as follows:

- Identification (ID), i.e.: each glacier entity has a unique identification code.
- Coordinates, i.e: we reported the coordinates describing the location of a glacier as accurately as possible.
- Date, i.e.: each glacier outline is associated with the date of its acquisition, if possible day, month and year.
- Surface area.
- Length, i.e.: we evaluated and inserted for each glacier the longest flowline value.
- Minimum elevation.
- Maximum elevation.
- Mean elevation.
- Median elevation.

– Mean orientation/aspect. We derived the mean aspect from a DTM, that allows one to consider the value of all individual cells that are covered by the glacier and to derive a mean value in the full 0–360° range.

– Slope, i.e.: the mean slope was derived from elevation range and glacier length.

The images used in this study are from Landsat TM and ETM+ scenes of 2001 and 2010. Details of the scenes are provided in Table 1. For year 2001; Landast 7 ETM+ PAN-sharpened images were used as the base for the glacier delineation. The scenes have been selected to obtain the least snow and cloud coverage. For 2010 Landsat 5 TM scenes were used primarily, due to problems with scan-line errors in the ETM+ scenes. Landsat 7 ETM+ gap-filled and PAN-sharpened images were simply used as a support, whenever it was not possible to recognize some parts of the glacier boundaries in the reference Landsat 5 scene (e.g. when hidden by shadows). Moreover, a Digital Elevation Model (DEM) from the Shuttle Radar Topography Mission (SRTM3) was used to extract elevation related glacial parameters (e.g. minimum, maximum and mean elevation, hypsography). We used the void filled CGIAR-CSI SRTM DEM version 4 (CGIAR-CSI, 2012), also used in other glacier related studies (Bolch et al., 2010). The co-registration of the Landsat scenes to the DEM resulted in a correlation of less than one pixel and thus no orthoprojection of the satellite images was needed.

To obtain glacier outlines we applied a semi-automatic approach. A fully automatic classification system was not suitable since there are three main factors making glacier boundary assessment uncertain, namely (i) debris cover, (ii) attached seasonal and/or perennial snow, and (iii) the position of drainage divides in the accumulation area. Such items make the accuracy of the final classification largely driven by operator's sensitivity (ESA, 2013). Thus, additional manual classification was applied upon the automatic results. As a basis for the classification scheme we have used some band combinations, namely (i) 321 (true color), (ii) 543 (snow and ice represented by blue), and (iii) band ratios 4 and 5 (TM4/TM5). A Supervised Maximum Likelihood (SML) classification was initially used to detect all classes (bare-ice, debris, snow, rocks, shadows) in the study

area, but it displayed poor accuracy. A comparison of the results of SML with the true color image (band 321) showed large differences between automatic classification and manual identification of specific classes. Eventually, we could use SML only to identify shadow areas, that were mostly excluded from further analysis. The combination of different image products gave the best resulting glacier maps. Band combination 543 allowed a clear delineation of snow and ice, the ratio TM4/TM5 provided detection of the limits of snow accumulation areas (in particular upon the image acquired on 30 September 2001), while the true color image was used for detection of supraglacial debris, and for quality check of classification. In addition, we evaluated our results against our DEM and slope maps, which also supported the detection of morphological evidence of debris covered ice, thus allowing to properly identify glacier snouts and termini whenever covered by supra-glacial debris. We also referred to Google Earth© to analyze high resolution SPOT images from the study area. After successful delineation of the glacier boundaries, the area of each polygon was computed using a Geographic Information System (GIS) software. Other glaciological parameters, such as minimum, maximum and mean elevation, and the hypsographic curves, have been obtained by combining the glacier outlines with the DEM.

3.1.2 Glacier outlines accuracy and error assessment

When performing a temporal analysis, inaccuracies may occur due to positional and mapping errors. The latter depend upon the image resolution and its conditions at the time of acquisition, namely cloud and snow-cover, presence of shadows and debris hampering ice detection.

1. Georeferencing error

This type of error depends upon the referencing quality with respect to the specific projection system. For our study we chose level 1T as the best possible one for georeferencing. The georeferencing accuracy of this type of data is obtained by NASA, delivering the product, by means of a correction process based both upon Ground

Control Points (GCPs, taken from the 2005 Global Land Survey), and Shuttle Radar Topographic Mission (SRTM) DEMs (Landsat7_Handbook, 2013). The SRTM DEM is thought to have good accuracy (Falorni et al., 2005, quoted also by Bolch et al., 2010), and it is more accurate in areas with low contrast. Visual inspection of the two overlapped images revealed a good match. Thus we considered this error negligible with respect to the other errors.

2. Linear resolution error (LRE)

Image resolution influences the accuracy of glacier mapping. The higher the resolution, the better the outlines, the smaller the error. Following Vögtle and Schilling (1999) and Citterio et al. (2007), the final planimetric precision value was evaluated considering both the uncertainty due to the sources (satellite images) and the clarity of glacier limits. The area precision for each glacier was evaluated by buffering the glacier perimeter considering the area uncertainty. The final precision of the whole CKNP glacier coverage was determined by taking the root of the squared sum of all the buffer areas. The error in area change ΔAE was then calculated as:

$$\Delta AE = \sqrt{\left(\sum_{i=1}^{711} P_{i,2001} \cdot LRE_{2001}\right)^2 + \left(\sum_{j=1}^{707} P_{i,2010} \cdot LRE_{2010}\right)^2} \quad (1)$$

Where $P_{i,2001}$ and $P_{j,2010}$ are the glacier perimeters, and i/j is the number of analyzed glaciers, for 2001 and 2010 respectively, ranging from 1 to 711/707, respectively. LRE_{2001} is the Linear Resolution Error affecting 2001 Landsat images while LRE_{2010} is that of 2010. As suggested by O'Gorman (1996), the precision error is half a pixel for the area delineation. Therefore, the LRE should be half the resolution of a single image, i.e. in our case 7.5 m for the 2001 scene (the resolution of which was previously implemented by the PAN-*sharpening* technique), and 15 m for the most recent one.

3. Errors depending on specific scene conditions

Seasonal snow, cloud cover and presence of shadows and debris can introduce errors in glacier area determination. Therefore, we selected scenes with the least possible snow and cloud cover (the latter is less than 6 %). Concerning snow cover, we minimized its impact by choosing the LANDSAT images where glacier ablation area was as snow-free as possible, and according to their temporal coherence, so as to avoid major differences between the scenes for the same year (similar seasonality, see Table 1). We also referred to other sources (SPOT from Google Earth©) whenever certain glacier features were not visible in the Landsat images. Furthermore, we used SML classification to identify shadow areas, that were mostly excluded from the analysis.

3.1.3 Supraglacial debris-coverage

We applied a Supervised Maximum Likelihood (SML) classification to the Landsat false colour composite image (i.e.: 543 bands) to map the supraglacial debris upon the study area in 2001 and 2010. We first extracted the glacial areas upon the 2001 glacier mask, thus reducing possible misclassifications in the classifier-training, due to out-of-glacier pixel noise.

We chose to consider only glaciers larger than 2 km^2, because Landsat resolution was too poor to discriminate debris areas in very small glaciers. So doing, we considered 4273 km^2 of ice cover (ca. 95 % of the total area). We then trained the classifier to discriminate between two classes ("clean-ice" and "supraglacial debris"), by choosing appropriate Region of Interests (ROIs). This led to an accurate automatic classification of the debris, validated then by visual comparison of the resulting debris masks against the visible colour Landsat images. We then investigated the debris cover change within the studied period (2001–2010). Eventually, to investigate the role of debris cover within glacier ablation area, we set the highest line of ablation to 5200 m a.s.l. (see e.g. Bocchiola et al., 2011).

3.1.4 Debris mapping accuracy

Equation (1) was also applied to evaluate the error affecting debris-mapping. LREs were the same used for glacier outlines accuracy assessment (namely 7.5 m for 2001 and 15 m for 2010).

3.2 Snow cover data

3.2.1 Snow detection

We used MODIS images to investigate snow-cover variability during 2001–2011 within the CKNP. We downloaded the MOD10A2-V5 product, i.e. pre-processed raw MODIS images, showing snow and other environmental features (e.g. lakes, clouds, etc.), freely available from the National Snow and Ice Data Center website (NSDIC, 2013). The data set contains fields of maximum snow cover extent over an eight-day period (bundle). All the images have undergone further processing to fit the study area, and a threshold for cloud cover was set to reduce clouds noise over the scenes. The overall process consists of different steps:

- Re-projection from Sinusoidal to WGS84 Zone 43N projection;
- Image clipping to fit CKNP area;
- Attribute Tables extraction;
- Table and MODIS scene filenames export to spreadsheet.

All these steps have been cascaded into a script to process all data batch using Python language (Python, 2013) combined with a GIS. Cloud coverage was inspected first considering different thresholds, and a best output was taken as a tradeoff between data quality and quantity. In fact, the lower the threshold, the cleaner the scenes, but with a higher loss of area. On the other hand, too high a threshold would lead to poor quality. Thus we set the threshold to 50 %, as a best tradeoff. Most of the available dataset

have not yet been investigated by the NSDIC group for quality check, and further analyses are ongoing. We compared our results against those in Tahir et al. (2011), that studied snow-cover in the Hunza basin, north of the CKNP. We investigated snow cover changes per elevation belts (A, B, C), trying to match as much as possible those reported by Tahir et al. (2011). The classification is shown in Table 2.

We carried out linear regression of snow cover data within the three selected altitude belts. To provide a meaningful comparison between different years, we chose to compare snow cover at fixed dates. Within the available database of reasonably clear images we chose a number of dates where images were available for several years. We selected five dates during ablation season (from 18 June to 30 September), and a total of 37 images. We chose to analyze dates during the ablation season because a significant analysis of the accumulation season (fall–spring) would not have been possible due to lack of a sufficient amount of data. Also, glacier nourishment is related to snow accumulation at onset of thaw season and snow depletion thenceforth, so the considered period seems relevant. Given the short series (11 yr) of snow cover data, neither we carried out significance analysis of the observed trends, nor we pursued other statistical tests (e.g. Mann–Kendall).

3.2.2 Snow data accuracy

As summarized in Parajka and Blöschl (2012), most of the MODIS accuracy assessments reported the overall accuracy between 85 % and 99 % during clear sky conditions. The accuracies at individual sites vary between 87.5 % and 100 %, but there is no clear dependence between mapping accuracy and topography (Parajka et al., 2012). Moreover, Tahir et al. (2011) have used ASTER images (which have high-spatial resolution) to validate MODIS snow cover products in the Hunza basin. The results they obtained suggest that MODIS snow products are accurate in estimating snow cover within our study area.

3.3 Climate data analysis

We investigated monthly averaged meteorological variables, kindly provided by the Pakistan Meteorological Department (PMD), derived from measurements at a number of stations in North Eastern Pakistan during 1980–2009. Data from the three closest stations to the CKNP area, namely Gilgit, Bunji and Astore (from North to South, Fig. 1) are used for this study. Earlier investigations (Weiers, 1995; Winiger et al., 2005; Bocchiola and Diolaiuti, 2013), suggested that in Northern Pakistan three main climatic regions can be identified, depending mainly upon characteristic rainfall regimes. These are

1. Western Himalaya (Kaghan Valley and Nanga Parbat), marginally influenced by the monsoon, with annual precipitation ranging from 900 to 1300 mm in the altitudinal range between 1000 and 4000 m a.s.l., and increasing to 2300 mm at 5500 m a.s.l.,
2. Chitral–Hindukush, influenced by Mediterranean low pressure systems in winter and spring, with average annual precipitation from 500 mm at 1000 m a.s.l. to 1300 mm at 5500 m a.s.l., and
3. Northwest Karakoram (including the CKNP area), with winter and occasional spring and summer rainfall, where precipitation increases from 150–500 mm at 1500–3000 m a.s.l. to more than 1700 mm at 5500 m a.s.l.

All three meteorological stations used here are nested into Northwest Karakoram region. The analysis covers seasonal values of total precipitation, number of wet days and maximum and minimum air temperature. The data are investigated for trends with linear regression (LR) analysis and the non-parametric Mann–Kendall (MK) test, both traditional and progressive (backward–forward). MK highlights not linear trends, and may pinpoint the onset period of a trend, if any (Bocchiola and Diolaiuti, 2010). The station altitudes range from 1460 m a.s.l. (Gilgit) to 2168 m a.s.l. (Astore), which is rather low in comparison with the hypsography of the region and the likely large precipitation

gradient in higher altitudes (Winiger et al., 2005; Wulf et al., 2010; Bocchiola et al., 2011). Data from automatic weather stations (AWSs) at higher altitudes (e.g. Askole, 3015 m a.s.l., and Urdukas, 3926 m a.s.l., installed by EVK2CNR committee, see Bocchiola et al., 2011) are available, but for very short periods (2005–now). Eventually, the three chosen stations are the only ones available in our knowledge to analyse recent climate patterns within the CKNP area. Given the relative proximity to the CKNP (Gilgit and Bunji are placed 10–20 km from CKNP boundaries, Astore ca. 50 km), the climate data within the selected stations may be thought as representative of climate within the park area. Also, in spite of the considerable vertical gradients within the area (temperature and precipitation, the latter more uncertain), relative variations observed at the selected stations may be taken as representative of variation also at the highest altitudes, at least in a first approximation.

Unfortunately, no snow gauges are available in the PMD data base, so no direct inference can be made about snow amount and snow water equivalent SWE (see. e.g. Bocchiola and Rosso, 2007; Bocchiola, 2010; Bocchiola and Groppelli, 2010; Diolaiuti et al., 2011, 2012), but only indirectly through remote sensing of snow covered area SCA, like we do here, and hydrological modeling (see e.g. Bocchiola et al., 2011). The main parameters for the climate analysis are the monthly amount of precipitation P_m (mm), the monthly number of wet days D_w, the monthly average of the maximum and minimum day-time air temperature T_{max} (°C), T_{min} (°C). P_m provides the hydrological input on the area, while D_w indirectly indicates the frequency (or average duration) of precipitation events (days with rainfall). No information concerning splitting of precipitation into either rainfall or snowfall is available here, and P_m is labeled as "monthly amount of precipitation". Upon analysis of the average winter temperature, that are below zero in several sites, and of considerable P_m values during winter unlikely to represent entirely liquid values, we assume here that water under snowfall is included here and P_m is a measure of total precipitation. The maximum and minimum day-time temperatures, T_{max} and T_{min}, provide indication about the temperature characteristics in the investigated periods (e.g. arrival and duration of heat waves). Annual and seasonal (JFM,

etc.) values of the variables are also derived and used in the analysis, and $P_{m,Y/SEA}$ is the sum of the monthly values during a year/season, $D_{w,Y/SEA}$ represents the mean of monthly values during a year/season, and $T_{max,Y/SEA}$ and $T_{min,Y/SEA}$ are calculated as the mean of monthly values during a year/season.

The significance of LR during the period of observations is given by the p-value ($\alpha = 5\,\%$, e.g. Jiang et al., 2007). Multiple trends could be identified in the time series analysis, e.g. by assessing slope changes (see e.g. Seidou and Ouarda, 2007). However, in view of the relative shortness of the series here, a single slope regression analysis is carried out. The Mann–Kendall test (Mann, 1945; Kendall, 1975) is widely adopted to assess the significance of trends in time series (Hirsch and Slack, 1984; Gan, 1998; Chiew and McMahon, 1993; Lettenmaier et al., 1994; Zhang et al., 2000; Yue and Wang, 2002; Bocchiola et al., 2008). It is a non-parametric test, less sensitive to extreme values, and independent from the hypothesis about the nature of the trend (e.g. Wang et al., 2005). Consider a sample of a random variable, e.g. P_m, $\{ P_{m,y}, y = 1,2,\ldots,Y \}$ with Y being the length of the series. Taken a value within the sample with index y, we define p_y as the number of elements of the sample with $j < y$ for which $P_{m,j} < P_{m,y}$. Then τ is defined as

$$\tau = \sum_{y=1}^{Y} p_y. \tag{2}$$

It turns out that τ is asymptotically normally distributed, and its mean and standard deviation are

$$\mu(\tau) = Y(Y-1)/4; \quad \sigma(\tau) = \sqrt{Y(Y-1)(2Y+5)/72}. \tag{3}$$

The variable $u(\tau) = (\tau - \mu(\tau))/\sigma(\tau)$ is then a standard normal, and it is possible to derive the associated confidence interval. The Mann–Kendall test verifies the assumption of stationarity by investigating if $u(\tau)$ is within the confidence interval for a given significance level (e.g. for $\alpha = 5\,\%$, the range would be -1.96 to 1.96). In the progressive

form of the Mann–Kendall test, the variables τ_j and $u(\tau_j)$ are calculated for each element of the sample j, by trading Y for j in Eqs. (2) and (3). The value of τ defines the direction (positive/negative) and magnitude (modulus) of the trend. The same procedure is applied by starting from the most recent values and backward. In this case, p'_i indicates the number of elements of the series of $P_{m,y}$ with $j > y$, and $P_{m,j} > P_{m,y}$. Then $u(\tau'_j)$ is calculated accordingly from p'_y and τ'_j. If no trend is present, the diagram of $u(\tau_j)$ and $u(\tau'_j)$ against the sample unit (e.g. time) shows several crossing points. Contrarily, if the series is affected by a trend, the crossing period is unique and allows to approximately locate the starting point. Here the MK test was applied to raw data, without pre-whitening, according to Yue and Wang (2002). Then, we investigated the correlation of the weather variables against the anomaly (vs. long term average) of the Northern Atlantic Oscillation (NAO) index (e.g. Hurrell, 1995; Jones et al., 1997; Osborn, 2004, 2006), during 1980–2009. Archer and Fowler (2004) obtained a statistically significant (positive) correlation between winter precipitation and a monthly index (November to January) of the NAO during 1961–1999, and a significant negative correlation between NAO and summer rainfall at several stations. Further on, we tried and verify the hypothesis that the temperature evolution in the Karakoram is related to warming at global or hemispheric scale. To do so, we investigated the correlation between global temperature anomalies DT_G (calculated according to Brohan et al., 2006) and T_{min} and T_{max} of the station data.

4 Results

4.1 The CKNP glacier changes during 2001–2010

The 2001 inventory displayed 711 glaciers within the CKNP region (Table 5). Their total area is 4587 ($\pm 18\,km^2$), namely $\sim 38\,\%$ of the total surface of the Central Karakoram National Park ($12\,162\,km^2$) and 35 % of the surface of our study area ($13\,199\,km^2$). This area represents $\sim 30\,\%$ of the glacier surface of the entire Karakoram range in

Pakistan (total area from ICIMOD, 2012). Thus, the CKNP glaciation seems a representative sample for future considerations upon glaciers in upper Pakistan. The biggest glacier is 604 km^2 large (i.e. Baltoro), while the overall average glacier size is 6.5 km^2. The 9 largest glaciers (1.27 % of the total number) cover more than half of the glacierized surface. The smallest glaciers class (433 glaciers < 1 km^2) covers ca. 61 % of all glaciers by number, while covering only 3.6 % of the glacier surface (see Table 6). Fifty-three glaciers had an area smaller than 0.1 km^2 in 2001. Nevertheless they all together covered a surface area of 2 km^2 and were integrated in the CKNP Glacier Inventory as "glacierets". The glacier minimum elevation (i.e.: glacier terminus altitude) was between 4500 and 5000 m a.s.l. for almost 40 % in number of all the mapped glaciers. On the other hand, this share of glaciers only accounts for 5 % of ice cover overall. In fact, almost half of the glacier area is covered by a few bigger glaciers (only the 3.4 % of the total number), with a minimum elevation between 3000 and 3500 m a.s.l. (see Tab. 4). This mirrors the fact that larger glaciers tend to reach lower elevations, while smaller glaciers have higher termini, as observed in other glaciated regions, including Alaska Brooks Range (Manley, 2005), Swiss glaciers (Kääb et al., 2002), Cordillera Blanca (Racoviteanu et al., 2008a), and Italian Alps (Diolaiuti et al., 2011, 2012a,b).

Our mapped glaciers were sorted according to the size classes introduced by Bolch et al. (2011), who studied Garhwal Himalaya's glaciers in India. They applied size classes as follows: < 0.5 km^2, 0.51–1.0 km^2, 1.01–2.0 km^2, 2.01–5.0 km^2, 5.01–10.0 km^2, 10.01–20.0 km^2, 20.01–50.0 km^2, > 50.01 km^2(Table 5). The hypsography of the glacierized areas (2001) for the size classes and 100 m elevation belts is shown in Fig. 2 (based on the SRTM DEM of 2000). The glaciers range in elevation from 2250 to 7900 m a.s.l.

The glacier size displays some characteristic distribution against glaciers' altitude (Fig. 3). Small glaciers with an area less than 1 km^2 are restricted to elevations above 3500 m a.s.l.. The elevation range is not very large, but some of the small glaciers are found at up to 7000 m a.s.l.

We found a significant relationship (ρ = 0.5) between the area and the vertical extent of the glacier (i.e. difference between maximum and median elevation). Glaciers with small vertical extent (i.e. maximum elevation close to median) feature small areas. In addition, we found a significant relationship (ρ = 0.5) of the area vs. the altitudinal range (i.e. maximum minus minimum elevation).

Then correlation analysis showed that small glaciers possess both smaller altitudinal range and vertical extent. Conversely larger glaciers possess wider altitudinal range and vertical extent and their snout reach the lower elevations. Most of the large and prominent glaciers originate above 7000 m a.s.l. and have wide elevation range. Moreover, the minimum elevation reached by some of these large glaciers is much lower than in the Greater Himalaya of India and Nepal (Hewitt, 2005). It is also interesting to note that the mean elevation of all glaciers sizes is ca. 4990 m a.s.l., i.e. only a few hundred meters below the estimated ELA.

In the inventory of 2010 the number of glaciers is slightly lower than in 2001, with 707 glaciers (due to some individual glaciers advancing to merge with neighboring glacier bodies, see also Fig. 5), covering an area of 4613 km^2 (±38 km^2). Their size distribution is shown in Table 5. Some glaciers have shifted from one size class to another during 2001–2010. To avoid inconsistencies, Table 6 shows the contribution of each glacier according to the class it belonged to in 2001.

Based on this analysis, the total glacier surface increased slightly, by ca. 27 km^2 during 2001–2010. The relative area change is not remarkable (+0.6 % of the 2001 area), and it is smaller than the error we calculated from Eq. (1) (±42 km^2), thus suggesting rather stable conditions. Moreover, we found 40 glaciers (over the whole sample of more than 700) with changed area, i.e. only 0.06 % of the CKNP glaciers varied its surface, confirming the stability of this glacierized region.

In spite of the overall stable situation, when focusing upon those 40 glaciers witnessing surface change (i.e. due to advance or surge events), noticeable variations are found (Fig. 6a, b). Especially glaciers in the size classes from 10 to 50 km^2 have shown appreciable advances, with a decrease of the minimum elevation of up to 60 m

with respect to 2001. These advances consisted in a downshift of the glacier minimum elevation in 2010. In some cases they even advanced on top of their bigger neighboring glaciers. A most prominent example is given by Panmah's tributaries, some of which have experienced surges from 2001 and 2005 (Hewitt, 2007), now protruding far onto the main trunk of the Panmah glacier, which may (Fig. 6a) or may not (Fig. 6b) result into a surface area increase.

Our results are in agreement with earlier observations, e.g. by Hewitt (2005), claiming the existence of the "Karakoram anomaly", a regional deviation from the general glacier shrinkage observed in most glacierized areas worldwide (e.g. Gardelle et al., 2012). Other neighboring Asian glacierized areas are undergoing a general glacier decline (IPCC, 2007; Bolch et al., 2010; Bhambri et al., 2011; Pan et al., 2012), thus indicating different conditions in the Karakoram.

Here, we distinguished glacier-snout movements between advancing and surging type by visual inspection of the Landsat scenes. We focused upon the magnitude of glacier-termini advance, and we labeled it as a surging type when it exceeded about $150\,m\,yr^{-1}$ (Cuffey and Paterson, 2010). Under this assumption, and according to the present literature (Hewitt, 2007; Copland et al., 2011), 6 glaciers (Panmah and Braldu glaciers and some of their tributaries) are potentially affected by actual surge phenomena. Furthermore, looped moraines are present on their surfaces, supporting this hypothesis (Copland et al., 2003). Then the rest (and most) of glacier expansion through recent years could be charged upon diffuse glacier advance activity. Barrand and Murray (2006) analysed 150 glaciers in the Karakoram, using multivariate statistical analysis of data derived from ASTER and Landsat. They found that the incidence of surging was statistically connected to various size-related variables, including glacier length and perimeter, and debris cover. Moreover, the effect of glacier perimeter upon surging may be explained by the increased availability of avalanche-fed snow and debris material which may act as a mass balance proxy. In our case, the 6 glaciers witnessing surge-type advances show complex perimeters, but not abundant supraglacial debris.

4.2 Debris-cover changes during 2001–2010

Landsat images displayed that the total supraglacial-debris-coverage was $977\,km^2$ ($\pm 138\,km^2$) in 2001, and $1070\,km^2$ ($\pm 194\,km^2$) in 2010, about 20 % of the total ice covered area. When considering only the ablation area, the percentage rose up to 31 %. The accuracy of the surface comparison is $\pm 238\,km^2$, then the change in the debris cover area of $+92\,km^2$ falls within the error range. In spite of this non-significant area change, debris cover increment can be appreciated by comparison of two FCC images upon some selected glaciers (Fig. 7). Source of debris cover may have been rocky avalanches due to steep slopes, glacier dynamics, wind action and other factors. The maximum cover was found at 4300 m a.s.l., in the ablation zone. Supraglacial debris increase is likely another cause of the stable conditions of the Karakoram glaciers. In fact supraglacial debris coverage, whenever thicker than the "critical thickness" (*sensu* Mattson et al., 1993), is proven to reduce buried ice melting rates (Mihalcea et al., 2006).

4.3 Snow-cover variability during 2001–2010

We analyzed trends of snow cover data during 2001–2010 (see Fig. 8). An increasing trend of snow cover is seen through time in all the elevation belts (Table 2). In Belt A, a gain of $+0.09\,km^2\,yr^{-1}$ was observed, or 2 % of snow cover area yearly. In Belt B, snow cover area increased by $+2.35\,km^2\,yr^{-1}$, or $+0.6\,\%\,yr^{-1}$. Belt C has increasing snow cover of $+14.86\,km^2\,yr^{-1}$, or $+0.2\,\%\,yr^{-1}$. These results are qualitatively similar to those in Tahir et al. (2001), who studied snow variability of the Hunza basin during 2001–2009, finding increasing snow cover area, especially in Belt C during summer.

4.4 Climate trends in the period 1980–2009

The results of the trend analysis of climate are shown in Table 7. The progressive MK test was carried out whenever both MK and LR tests showed non-stationarity. The

results of this analysis, i.e. onset date, and average values before and after this date, as compared to long term average, are also reported in Table 7. Especially P_m demonstrates a substantial stationary behavior, and no significant change of total precipitation is seen in the area. Concerning the number of wet days (D_w), increasing values are found in Gilgit (yearly, *Y* since 2001, JFM with no clear onset), i.e. there is a significant increase of the number of yearly (and winter) precipitation events. In Astore significant increase of D_w is found in summer months (JAS) via the LR test. In Bunji non-significant decreasing values are observed. The minimum temperature T_{min} increases significantly in Astore for winter and spring (JFM, AMJ, since 1999–2002) and in Bunji also for all periods except in summer (*Y*, JFM, AMJ, OND, since 1997–2003). In Gilgit T_{min} decreases significantly during summer (JAS, since 1986), while a non-significant decrease is found in fall and yearly. The maximum temperature T_{max} increases significantly yearly, in fall and winter in Astore (*Y* since 1998, Fig. 3, JFM since 2000). Also in Gilgit significant T_{max} increases are observed for most periods (*Y*, JFM, since 1995, OND, since 1991), while Bunji shows a significant T_{max} increase only in winter (JFM, since 1997) and a non-significant decreasing trend in JAS. We then evaluated the (linear) correlation between (i) local temperatures and global thermal anomalies, and (ii) the investigated weather variables and the NAO index. As a representative parameters of the region, the averaged values between the three stations have been used (Table 7). The minimum air temperature T_{min} is slightly, but significantly positively correlated with respect to DT_G yearly, in winter and spring. The maximum air temperature T_{max} is significantly positively correlated against DT_G for annual as well as seasonal periods, especially in fall and winter. Concerning the NAO index, P_m shows a significant correlation (negative vs. *Y*, and positive vs. JAS and OND), but small in absolute value. The duration of wet periods D_w is significantly shorter for higher NAO anomalies, unless during spring. The minimum temperature T_{min} is negatively correlated to NAO during winter and spring. T_{max} is negatively correlated to NAO (*Y*, JFM, AMJ).

5 Discussion and conclusion

We used remote sensing data of ice and snow cover, together with climate data from PMD automatic weather stations, to provide an overview of the state of glaciers within CKNP in northern Pakistan, and possible trends occurring lately.

From our glacier inventory, in 2001 CKNP glaciers covered an area of 4587 (±18 km^2), namely ∼ 38 % of the park surface and ∼ 30 % of the glacier surface of the entire Karakoram range in Pakistan. In 2010 we found an ice coverage of 4613 km^2 (±38 km^2), thus giving a not remarkable area change (+0.6 % of the 2001 area), which is also smaller than the error affecting our computation (±42 km^2), thus suggesting rather stable glacier conditions.

Moreover, we found 40 glaciers (over the whole sample of more than 700) with changed area, i.e. only 0.06 % of our glaciers was found varying its surface, thus confirming the stability of this glacierized region.

Nevertheless, when focusing on this small subset of changing glaciers noticeable variations can be detected. Especially glaciers in the size classes from 10 to 50 km^2 have shown appreciable advances, with a decrease of the minimum elevation of up to 60 m with respect to 2001. These advances consisted in a downshift of the glacier minimum elevation in 2010. In some cases they even advanced on top of their bigger neighboring glaciers (mostly because of actual snout advances and few because of surges).

The most prominent examples of surging glaciers are given by Panmah's tributaries, some of which have experienced surges from 2001 and 2005 (Hewitt, 2007), now protruding far onto the main trunk of the Panmah glacier (Fig. 6).

The supraglacial debris was found 977 km^2 (±138 km^2) in 2001, and 1070 km^2 (±194 km^2) in 2010, about 20 % of the total ice covered area and 31 % of the ablation area. This debris coverage may have played a role in maintaining the quite stable conditions of the Karakoram glaciers. In fact, supraglacial debris can decrease ice melting rate (i.e. whenever thicker than the "critical value", see Mattson et al., 1993).The

surface change falls within the error range affecting our calculation ($\pm 238\,km^2$) but it is clearly appreciable by analysing FCC images upon some selected glaciers, suggesting it really happened (Fig. 7).

We found snow cover increase at thaw (June–September) everywhere. Our climate analysis revealed a significant decrease in minimum summer temperatures ($-1.5\,^{\circ}C$ during 1980–2009) at Gilgit, and a general increase in winter wet days ($+3.3\,days\,yr^{-1}$ during 1980–2009), which at high altitudes might have supported the increase of snow cover as detected. This favourable climate behaviour, together with the peculiar glacier setting, with the largest part of ice bodies above 4500 m a.s.l. and a large fraction of the melting glacier surface covered by rock debris, may have caused small ice losses. These factors may have resulted into the stable ice cover area we found.

These findings are in agreement with the evidence of the "Karakoram anomaly" (Hewitt, 2005), a regional deviation from the general glacier shrinkage observed in most glacierized zones worldwide, and also agree with the results by Kääb et al. (2012). This glacier "anomaly" was only partially affected by glacier surges, unlikely to be a main cause of glaciers' snout advance.

Our findings are also in agreement with Gardelle et al. (2012, 2013) who used satellite data to find out a slight mass gain for the glaciers of this area, and estimated the Karakoram mass balance to be $+0.10 \pm 0.19\,m\,yr^{-1}$ water equivalent.

To further deepen knowledge of glaciers evolution in our target region more field data are required, especially to describe high resolution glacier changes (glacier mass balances), and to evaluate magnitude and rate of snow accumulation. The lack of snow depth data at the highest altitudes, terribly important for ice nourishing, may limit our understanding of glaciers' dynamics, and claims for further investigation in this sense. Extensive field data collection could improve our knowledge of behavior and dynamics of glaciers in this part of the "Third Pole".

Acknowledgements. Landsat data used in this paper are distributed by the Land Processes Distributed Active Archive Center (LP DAAC), located at USGS/EROS, Sioux Falls, SD, http://lpdaac.usgs.gov.

Climate data are kindly provided by PMD (Pakistani Meteorological Department).

This research was performed under the umbrella of SEED and PAPRIKA projects.

SEED is a project funded by Pakistani and Italian governments, and managed by EvK2-CNR Committee.

PAPRIKA is a project funded and managed by EvK2-CNR Committee (it is the twin project of the PAPRIKA France program).

References

Ageta, Y. and Higuchi, K.: Estimation of mass balance components of a summer accumulation type glacier in Nepal, Himalaya, Geogr. Ann. A, 66A, 249–255, 1984.

Ageta, Y. and Fujita, K.: Characteristics of mass balance of summer – accumulation type glaciers in the Himalayas and Tibetan Plateau, Zeitschrift für Gletscherkunde und Glazialgeologie, 32, 61–65, 1996.

Aggarwal, P. K., Joshi, P. K., Ingram, J. S. I., and Gupta, R. K.: Adapting food systems of the Indo–Gangetic plains to global environmental change: key information needs to improve policy formulation, Environ. Sci. Policy, 7, 487–498, 2004.

Akhtar, M., Ahmad, N., and Booij, M. J.: The impact of climate change on the water resources of Hindukush–Karakoram–Himalaya region under different glacier coverage scenario, J. Hydrol., 355, 148–163, 2008.

Archer, D. R.: Contrasting hydrological regimes in the upper Indus Basin, J. Hydrol., 274, 198–210, 2003.

Archer, D. R. and Fowler, H. J.: Spatial and temporal variations in precipitation in the Upper Indus Basin, global teleconnections and hydrological implications, Hydrol. Earth Syst. Sci., 8, 47–61, doi:10.5194/hess-8-47-2004, 2004.

Barrand, N. and Murray, T.: Multivariate controls on the incidence of glacier surging in the Karakoram Himalaya, Arct. Antarct. Alp. Res., 38, 489–498, 2006.

Belò, M., Mayer, C., Lambrect, A., Smiraglia, C., and Tamburini, A.: The recent evolution of Liligo Glacier Karakoram, Pakistan and its present quiescent phase, Ann. Glaciol., 48, 171–176., 2008.

Bhambri, R., Bolch, T., Chaujar, R. K., and Kulshreshtha, S. C.: Glacier changes in the Garhwal Himalaya, India, from 1968 to 2006 based on remote sensing, J. Glaciol., 57, 534–556, 2011.

Bocchiola, D.: Regional estimation of Snow Water Equivalent using Kriging: a preliminary study within the Italian Alps, Geogr. Fis. Din. Quat., 33, 3–14, 2010.
Bocchiola, D. and Diolaiuti, G.: Evidence of climate change within the Adamello Glacier of Italy, Theor. App. Climat., 100, 3–4, 351–369, 2010.
Bocchiola, D. and Diolaiuti, G.: Recent (1980–2009) evidence of climate change in the upper Karakoram, Pakistan, Theor. Appl. Climatol., doi:10.1007/s00704-012-0803-y, 2013.
Bocchiola, D. and Groppelli, B.: Spatial estimation of Snow Water Equivalent at different dates within the Adamello Park of Italy, Cold Reg. Sci. Technol., 63, 97–109, 2010.
Bocchiola, D. and Rosso, R.: The distribution of daily Snow Water Equivalent in the Central Italian Alps, Adv. Water Resour., 30, 135–147, 2007
Bocchiola, D., Bianchi Janetti, E., Gorni, E., Marty, C., and Sovilla, B.: Regional evaluation of three day snow depth for avalanche hazard mapping in Switzerland, Nat. Hazards Earth Syst. Sci., 8, 685–705, doi:10.5194/nhess-8-685-2008, 2008.
Bocchiola, D., Diolaiuti, G., Soncini, A., Mihalcea, C., D'Agata, C., Mayer, C., Lambrecht, A., Rosso, R., and Smiraglia, C.: Prediction of future hydrological regimes in poorly gauged high altitude basins: the case study of the upper Indus, Pakistan, Hydrol. Earth Syst. Sci., 15, 2059–2075, doi:10.5194/hess-15-2059-2011, 2011.
Bolch, T., Yao, T., Kang, S., Buchroithner, M. F., Scherer, D., Maussion, F., Huintjes, E., and Schneider, C.: A glacier inventory for the western Nyainqentanglha Range and the Nam Co Basin, Tibet, and glacier changes 1976–2009, The Cryosphere, 4, 419–433, doi:10.5194/tc-4-419-2010, 2010.
Bolch, T., Pieczonka, T., and Benn, D. I.: Multi-decadal mass loss of glaciers in the Everest area (Nepal Himalaya) derived from stereo imagery, The Cryosphere, 5, 349–358, doi:10.5194/tc-5-349-2011, 2011.
Bookhagen, B. and Burbank, D. W.: Towards a complete Himalayan hydrologic budget: the spatiotemporal distribution of snow melt and rainfall and their impact on river discharge, J. Geophys. Res., 115, F03019, doi:10.1029/2009jf001426, 2010.
Brohan, P., Kennedy, J. J., Harris, I., Tett, S. F. B., and Jones, P. D.: Uncertainty estimates in regional and global observed temperature changes: a new dataset from 1850, J. Geophys. Res., 111, D12106, doi:10.1029/2005JD006548, 2006.
CGIAR-CSI, Consortium for Spatial Information: http://www.cgiar-csi.org, last access: 20 February 2012.

Chiew, F. H. S. and McMahon, T. A.: Detection of trend or change in annual flow of Australian rivers, Int. J. Climatol., 13, 643–653, 1993.
Citterio, M., Diolaiuti, G., Smiraglia, C., D'agata, C., Carnielli, T., Stella, G., and Siletto, G. B.: The fluctuations of Italian glaciers during the last century: a contribution to knowledge about Alpine glacier changes, Geogr. Ann. A, 89, 164–182, 2007.
Cogley, J. G.: Geodetic and direct mass-balance measurements: comparison and joint analysis, Ann. Glaciol., 50, 96–100, 2009.
Copland, L., Sharp, M. J., and Dowdeswell, J. A.: The distribution and flow characteristics of surge-type glaciers in the Canadian High Arctic, Ann. Glaciol., 36, 73–81, 2003.
Copland, L., Pope, S., Bishop, M., Schroder Jr., J. F., Clendon, P., Bush, A., Kamp, U., Seong, Y. B., and Owen, L.: Glacier velocities across the Central Karakoram, Ann. Glaciol., 50, 41–49, 2009.
Copland, L., Sylvestre, T., Bishop, M. P., Shroder, J. F., Seoung, Y. B., Owen, L. A., Bush, A., and Kamp, U.: Expanded and Recently Increased Glacier Surging in the Karakoram, Institute of Arctic and Alpine Reasearch (INSTAAR), University of Colorado, available at: http://www.bioone.org/doi/full/10.1657/1938-4246-43.4.503, 2011.
Cuffey, K. M. and Paterson, W. S. B.: The Physics of Glaciers, 4th Edn., ISBN: 9780123694614, Pergamon Press, Oxford, UK, 2010.
Desio, A.: Italian Expeditions to the Karakorum (K2) and Hindu Kush, in: Leader II, vol. 1, edited by: Marussi, A., E. J. Brill, Leiden, 1964.
Diolaiuti, G., Pecci, M., and Smiraglia, C.: Liligo Glacier (Karakoram): reconstruction of the recent history of a surge-type glacier, Ann. Glaciol., 36, 168–172, 2003.
Diolaiuti, G., Maragno, D., D'Agata, C., Smiraglia, C., and Bocchiola, D.: A contribution to the knowledge ofthe last fifty years of Alpine glacier history: the 1954–2003 area and geometry changes of Dosdè Piazzi glaciers (Lombardy–Alps, Italy), Prog. Phys. Geogr., 35, 161–182, 2011.
Diolaiuti, G., Bocchiola, D., D'agata, C., and Smiraglia, C.: Evidence of climate change impact upon glaciers' recession within the Italian Alps: the case of Lombardy glaciers, Theor. Appl. Climatol., 109, 429–445, doi:10.1007/s00704-012-0589-y, 2012a.
Diolaiuti, G., Bocchiola, D., Vagliasindi, M., D'agata, C., and Smiraglia, C.: The 1975–2005 glacier changes in Aosta Valley (Italy) and the relations with climate evolution, Prog. Phys. Geogr., 36, 764–785, doi:10.1177/0309133312456413, 2012b.

ESA, European Space Agency: http://www.esa-glaciers-cci.org/index.php?q=overview, last access: 15 April 2013.
Fowler, H. J. and Archer, D. R.: Conflicting signals of climatic change in the Upper Indus basin, J. Climate, 19, 4276–4293, 2006.
Fujita, K. and Nuimura, T.: Spatially heterogeneous wastage of Himalayan glaciers, P. Natl. Acad. Sci. USA, 108, 14011–14014, 2011.
Gan, T. Y.: Hydroclimatic trends and possible climatic warming in the Canadian prairies, Water Resour. Res., 34, 3009–3015, 1998.
Gardelle, J., Berthier, E., and Arnaud, Y.: Slight mass gain of Karakoram glaciers in the early twenty-first century, Nat. Geosci. Letters, 5, 322–325, doi:10.1038/NGEO1450, 2012.
Gardelle, J., Berthier, E., Arnaud, Y., and Kääb, A.: Region-wide glacier mass balances over the Pamir-Karakoram-Himalaya during 1999–2011, The Cryosphere Discuss., 7, 975–1028, doi:10.5194/tcd-7-975-2013, 2013.
Haeberli, W.: Integrated perception of glacier changes: a challenge of historical dimensions, in: Glacier Science and Environmental Change, edited by: Knight, P. G., Blackwell, Oxford, 423–430, 2006.
Hewitt, K.: The Karakoram Anomaly? Glacier expansion and the "elevation effect", Karakoram Himalaya, Mt. Res. Dev., 25, 332–340, 2005.
Hewitt, K.: Tributary glacier surges: an exceptional concentration at Panmah Glacier, Karakoram, Himalaya, J. Glaciol., 53, 181–188. doi:10.3189/172756507782202829, 2007.
Hirsch, R. M. and Slack, J. R.: Non-parametric trend test for seasonal data with serial dependence, Water Resour. Res., 20, 727–732, 1984.
Hurrell, J. W.: Decadal trends in the North Atlantic Oscillation regional temperatures and precipitation, Science, 269, 676–679, 1995.
Immerzeel, W. W., van Beek, L. P. H., and Bierkens, M. F. P.: Climate change will affect the Asian water towers, Science, 328, 1382–1385, 2010.
Intergovernmental Panel on Climate Change (IPCC): Climate Change, 2001, The Scientific Basis. Contribution of Working Group II to the Third Assessment Report of the Intergovernmental Panel on Climate Change, Cambridge University Press, Cambridge, 2001.
Intergovernmental Panel on Climate Change (IPCC): IPCC Fourth Assessment Report: Climate Change 2007, Synthesis Report (AR4), WMO-UNEP, Geneva, 2007.
Jiang, T., Su, B., and Hartmann, H.: Temporal and spatial trends of precipitation and river flow in the Yangtze River Basin, 1961–2000, Geomorphology, 85, 143–154, 2007.

Jones, P. D., Jonsson, T., and Wheeler, D.: Extension to the North Atlantic Oscillation using early instrumental pressure observations from Gibraltar and South–West Iceland, Int. J. Climatol., 17, 1433–1450, 1997.
Kääb, A., Paul, F., Maisch, M., Hoelzle, M., and Haeberli, W.: The new remote sensing derived Swiss glacier inventory: II. First results, Ann. Glaciol., 34, 362–366, 2002.
Kääb, A., Huggel, C., Fischer, L., Guex, S., Paul, F., Roer, I., Salzmann, N., Schlaefli, S., Schmutz, K., Schneider, D., Strozzi, T., and Weidmann, Y.: Remote sensing of glacier- and permafrost-related hazards in high mountains: an overview, Nat. Hazards Earth Syst. Sci., 5, 527–554, doi:10.5194/nhess-5-527-2005, 2005.
Kääb, A., Berthier, E., Nuth, C., Gardelle, J., and Arnaud, Y.: Contrasting patterns of early twenty-first-century glacier mass change in the Himalayas, Nature Letter, 488, 495–498, doi:10.1038/nature11324, 2012.
Kahlown, M. A., Raoof, A., Zubair, M., and Kemper, W. D.: Water use efficiency and economic feasibility of growing rice and wheat with sprinkler irrigation in the Indus Basin of Pakistan, Agr. Water Manage., 8, 292–298, 2007.
Kaser, G., Fountain, A., and Jansson, P.: A Manual for Monitoring the Mass Balance of Mountain Glaciers, International Hydrological Programme Technical Documents in Hydrology No. 59, UNESCO, Paris, 2003.
Kehrwald, N. M., Thompson, L. G., Tandong, Y., Mosley-Thompson, E., Schotterer, U., Alfimov, V., Beer, J., Eikenberg, J., and Davis, M. E.: Mass loss on Himalayan glacier endangers water resources, Geophys. Res. Lett., 35, L22503, doi:10.1029/2008GL035556, 2008.
Kendall, M. G.: Rank Correlation Methods, Oxford Univ. Press, New York, 1975.
Landsat7_Handbook: http://landsathandbook.gsfc.nasa.gov/, http://lpdaac.usgs.gov, last access: 17 April 2013.
Lettenmaier, D. P., Wood, E. F., and Wallis, J. R.: Hydro-climatological trends in the continental United States, 1948–88, J. Climate, 7, 586–607, 1994.
Manley, W. F.: Geospatial inventory and analysis of glaciers: a case study for the eastern Alaska Range, in: Satellite Image Atlas of Glaciers of the World, edited by: Williams Jr, R. S. and Ferrigno, J. G., Professional Paper 1386-K, K424–K439, US Geological Survey, 2005.
Mann, H. B.: Nonparametric tests against trend, Econometrica, 13, 245–259, 1945.
Mattson, L. E., Gardner, J. S., and Young, G. J.: Ablation on debris covered glaciers: an example from the Rakhiot Glacier, Punjab, Himalaya, in: Snow and Glacier Hydrology, Proc.

Kathmandu Symp., November 1992, edited by: Young, G. J., IAHS Publ. no. 218, IAHS Publishing, Wallingford, 289–296, 1993.
Mayer, C., Lambrecht, A., Belò, M, Smiraglia, C., and Diolaiuti, G.: Glaciological characteristics of the ablation zone of Baltoro Glacier, Karakoram, Ann. Glaciol., 43, 123–131, 2006.
Mayer, C., Fowler, A. C., Lambrecht, A., and Scharrer, K.: A surge of North Gasherbrum Glacier, Karakoram, China, J. Glaciol., 57, 904–916, 2011.
Mihalcea, C., Mayer, C., Diolaiuti, G., Lambrecht, A., Smiraglia, C., and Tartari, G.: Ice ablation and meteorological conditions on the debris covered area of Baltoro Glacier (Karakoram, Pakistan), Ann. Glaciol., 43, 292–300, 2006.
NSIDC, National Snow and Ice Data Center: http://nsidc.org, last access: 13 March 2013.
O'Gorman, L.: Subpixel precision of straight-edged shapes for registration and measurement, IEEE Transactions on Pattern Analysis and Machine Intelligence, 18, 746–751, doi:10.1109/34.506796, 1996.
Osborn, T. J.: Simulating the Winter North Atlantic Oscillation: the roles of internal variability and greenhouse gas forcing, Clim. Dynam., 22, 605–623, 2004.
Osborn, T. J.: Recent variations in the Winter North Atlantic Oscillation, Weather, 61, 353–355, 2006.
Pan, B. T., Zhang, G. L., Wang, J., Cao, B., Geng, H. P., Wang, J., Zhang, C., and Ji, Y. P.: Glacier changes from 1966–2009 in the Gongga Mountains, on the south-eastern margin of the Qinghai-Tibetan Plateau and their climatic forcing, The Cryosphere, 6, 1087–1101, doi:10.5194/tc-6-1087-2012, 2012.
Parajka, J. and Blöschl, G.: MODIS-based snow cover products, validation, and hydrologic applications, in: Multiscale Hydrologic Remote Sensing Perspectives and Applications, edited by: Chang, Y. and Ni-Bin, H., CRC Press, 185–212, Print ISBN 978-1-4398-7745-6, 2012.
Parajka, J., Holko, L., Kostka, Z., and Blöschl, G.: MODIS snow cover mapping accuracy in a small mountain catchment – comparison between open and forest sites, Hydrol. Earth Syst. Sci., 16, 2365–2377, doi:10.5194/hess-16-2365-2012, 2012.
Paul, F., Huggel, C., and Kääb, A.: Combining satellite multispectral image data and a digital elevation model for mapping debris-covered glaciers, Rem. Sens. Environ., 89, 510–518, 2004a.
Paul, F., Kääb, A., Maisch, M., Kellenberger, T., and Haeberli, W.: Rapid disintegration of Alpine glaciers observed with satellite data, Geophys. Res. Lett., 31, L21402, doi:10.1029/2004GL020816, 2004b.

Paul, F., Barry, R. G., Cogley, J. G., Frey, H., Haeberli, W., Ohmura, A., Ommanney, C. S. L., Raup, B., Rivera, A., and Zemp, M.: Guidelines for the compilation of glacier inventory data from digital sources, Ann. Glaciol., 50, 119–126, 2010.
Peel, M. C., Finlayson, B. L., and McMahon, T. A.: Updated world map of the Köppen-Geiger climate classification, Hydrol. Earth Syst. Sci., 11, 1633–1644, doi:10.5194/hess-11-1633-2007, 2007.
Python: http://www.python.org/, last access: 13 March 2013.
Racoviteanu, A. E., Arnaud, Y., Williams, M. W., and Ordonez, J.: Decadal changes in glacier parameters in the Cordillera Blanca, Peru, derived from remote sensing, J. Glaciol., 54, 499–510, 2008a.
Salerno, F., Buraschi, E., Bruccoleri, D., Tartari, G., and Smiraglia, C.: Glacier surface-area changes in Sagarmartha national park, Nepal, in the second half of the 20th century, by comparison of historical maps, J. Glaciol., 54, 738–752, 2008.
Seidou, O. and Ouarda, T. B. M. J.: Recursion-based multiple changepoint detection in multiple linear regression and application to river stream flows, Water Resour. Res., 43, W07404, doi:10.1029/2006WR005021, 2007.
Shroder, J. F., Jr., Owen, L. A., Seong, Y. B., Bishop, M. P., Bush, A., Caffee, M. W., Copland, L., Finkel, R. C., and Kamp, U.: The role of mass movements on landscape evolution in the Central Karakoram: Discussion and speculation, Quaternary International, 236, 34–47, doi:10.1016/j.quaint.2010.05.024, 2010
Smiraglia, C., Mayer, C., Mihalcea, C., Diolaiuti, G., Belò, M., and Vassena, G.: Ongoing variations of Himalayan and Karakoram glaciers as witnesses of global changes: recent studies of selected glaciers, Developments in Earth Surface Processes, 10, 235–248, 2007.
Tahir, A. A., Chevallier, P., Arnaud, Y., and Ahmad, B.: Snow cover dynamics and hydrological regime of the Hunza River basin, Karakoram Range, Northern Pakistan, Hydrol. Earth Syst. Sci., 15, 2275–2290, doi:10.5194/hess-15-2275-2011, 2011.
Vögtle, T. and Schilling, K. J.: Digitizing maps, in: GIS for Environmental Monitoring, edited by: Bähr, H.-P. and Vögtle, T., Schweizerbart, Stuttgart, Germany, 201–216, 1999.
Wang, W., Van Gelder, P. H. A. J. M., and Vrijling, J. K.: Trend and stationarity analysis for streamflow processes of rivers in western Europe in the 20th century, Proceedings: IWA International Conference on Water Economics, Statistics and Finance, Rethymno, Greece, 8–10 July, 2005.

Weiers, S.: Zur Klimatologie des NW-Karakoram und angrenzender Gebiete. Statistische Analysen unter Einbeziehung von Wettersatellitenbildern und eines Geographischen Information systems (GIS), Bonner Geographische Abhandlungen, 92, Geographisches Institut, Universitat Bonn, Bonn, Germany, 1995.

Winiger, M., Gumpert, M., and Yamout, H.: Karakoram–Hindukush–western Himalaya: assessing high-altitude water resources, Hydrol. Process., 19, 2329–2338, 2005.

World Glacier Monitoring Service (WGMS): available at: http://www.wgms.ch/dataexp.html, 2012.

Wulf, H., Bookhagen, B., and Scherler, D.: Seasonal precipitation gradients and their impact on fluvial sediment flux in the Northwest Himalaya, Geomorphology, 118, 13–21, 2010.

Yue, S. and Wang, C. Y.: Applicability of pre-whitening to eliminate the influence of serial correlation on the Mann–Kendall test, Water Resour. Res., 38, 4-1–4-7, doi:10.1029/2001WR000861, 2002.

Zhang, X., Vincent, L. A., Hogg, W. D., and Niitsoo, A.: Temperature and precipitation trends in Canada during the 20th century, Atmos. Ocean, 38, 395–429, 2000.

Table 1. Landsat imagery used for the analysis.

Date	Image type	Scene identification No.	Path/row	Resolution [m]	Cloud cover [%]
21 Jul 2001	ETM+	LE71480352001202SGS00	148/35	15	1.41
30 Sep 2001	ETM+	LE71490352001273EDC01	149/35	15	5.67
23 Jul 2010	TM	LT51480352010235KHC00	148/35	30	2.60
17 Nov 2010	TM	LT51490352010290KHC00	149/35	30	2.77

Table 2. Characteristics of the three elevation zones for snow cover. Slope is value of slope from linear regression analysis upon average snow cover (see section Results). $Slope_{\%w}$ is slope weighted upon snow cover area.

Zone	Elevation range [m]	$AREA_{zone}$ [km^2]	Slope [$km^2\,yr^{-1}$]	$Slope_{\%}$ [$\%\,yr^{-1}$]
A	1900–3300	845	0.09	2 %
B	3301–4300	2803	2.35	0.6 %
C	4301–8400	9551	14.86	0.2 %
$A_{TOT}/Slope_{\%w}()$		13 200	17.31	0.25 %

Table 3. Details for the weather stations used in the study and the mean annual precipitation amounts and temperature (1980–2009). See also Fig. 1.

Station	North [°]	East [°]	Altitude [m a.s.l.]	Average (P_Y) [mm]	Average (T_Y) [°C]
Astore	35.20′	74.54′	2168	485.88	9.85
Bunji	35.40′	74.38′	1372	161.33	17.33
Gilgit	35.55′	74.20′	1460	136.63	15.79

Table 4. Minimum glacier altitude based on the 2001 inventory data.

Minimum glacier altitude [m]	Glacier number	Area coverage [km^2]	% of total area	% of total number
2000–2500	3	106	2.31	0.42
2500–3000	12	634	13.82	1.69
3000–3500	24	2153	46.93	3.38
3500–4000	80	95	20.71	11.25
4000–4500	231	437	9.52	32.49
4500–5000	268	253	5.52	37.69
5000–5500	76	36	0.78	10.69
> 5500	17	19	0.42	2.39
Total	711	4587	100	100

Table 5. Number of glaciers within CKNP, sorted according to their area. Number of glaciers reported for two years (2001 and 2010).

Size class [km^2]	2001 glacier number	2010 glacier number	2001 glacier area distribution [%]	2010 glacier area distribution [%]	2001 glacier number distribution [%]	2010 glacier number distribution [%]
< 0.5	291	290	1.44	1.43	40.93	41.02
0.5–1.0	142	142	2.16	2.17	19.97	20.08
1.0–2.0	117	117	3.71	3.71	16.46	16.55
2.0–5.0	74	72	5.01	5.03	10.41	10.18
5.0–10.0	36	36	5.36	5.35	5.06	5.09
10.0–20.0	18	17	5.14	5.16	2.53	2.40
20.0–50.0	16	16	11.45	11.40	2.25	2.26
> 50.0	17	17	65.66	65.77	2.39	2.40
Total	711	707	100.00	100.00	100.00	100.00

Table 6. Area coverage of glaciers within the CKNP according to satellite images (2001 and 2010) (columns 2 and 3). Surface area changes of the CKNP glaciers during 2001–2010 (column 4). Surface area changes of CKNP glaciers with respect to their own class, and to total area (columns 5 and 6). The area changes are computed considering each glacier according to the class it belonged to in 2001.

Size class [km^2]	2001 area [km^2]	2010 area [km^2]	ΔA 2001–2010 [km^2]	% of class area lost	% of total area lost
< 0.5	66	66	−0.1	−0.1	−0.4
0.5–1.0	99	100	0.2	0.2	0.7
1.0–2.0	170	171	0.2	0.1	0.7
2.0–5.0	230	232	1.6	0.7	6.2
5.0–10.0	246	247	0.4	0.1	1.4
10.0–20.0	236	238	1.9	0.8	7.3
20.0–50.0	525	526	0.2	0.0	0.7
> 50.0	3012	3034	22.2	0.7	83.4
Total	4587 ± 18	4613 ± 38	26.6 ± 42	0.6	100

Table 7. Results of the climate trend analysis: (a) results of the LR and MK analysis. For MK, p value is displayed. The LR values are the linear regression coefficients (i.e. slope of the regression line), LR p is corresponding to p value. In bold significant p value ($\alpha = 5\,\%$) are given. (b) The beginning year and average values before and after the start for the trends derived from the progressive MK test are given. LT is the long term (1980–2009) average. (c) Correlation analysis of station mean climatic variables vs. global temperature anomalies DTG and NAO index. The significant correlation ($\alpha = 5\,\%$) results are displayed in bold.

(a) Station	P_m–D_w	P_Y	P_{JFM}	P_{AMJ}	P_{JAS}	P_{OND}	D_{wY}	D_{wJFM}	D_{wAMJ}	D_{wJAS}	D_{wOND}
Astore	MK	0.38	0.40	0.60	0.90	0.56	0.25	0.96	0.66	0.10	0.71
Astore	LR s	−2.22	−0.94	−0.39	0.00	−0.89	0.34	0.01	−0.01	0.08	0.03
Astore	LR p	0.43	0.55	0.84	1.00	0.49	0.22	0.71	0.87	0.04	0.27
Bunji	MK	0.90	0.42	0.99	0.99	0.84	0.84	0.38	0.38	0.68	0.79
Bunji	LR s	−0.32	0.29	−0.18	0.03	−0.47	−0.06	−0.01	−0.03	0.00	0.02
Bunji	LR p	0.82	0.49	0.84	0.96	0.39	0.81	0.85	0.44	0.94	0.28
Gilgit	MK	0.42	0.87	0.40	0.79	0.90	0.00	0.00	0.15	0.21	0.93
Gilgit	LR s	0.59	0.09	0.78	−0.07	−0.20	0.87	0.11	0.09	0.06	0.03
Gilgit	LR p	0.55	0.80	0.34	0.87	0.64	0.00	0.00	0.04	0.12	0.38
Station	T_{min}–T_{max}	T_Y	T_{JFM}	T_{AMJ}	T_{JAS}	T_{OND}	T_Y	T_{JFM}	T_{AMJ}	T_{JAS}	T_{OND}
Astore	MK	0.07	0.05	0.04	0.71	0.23	0.01	0.01	0.34	0.99	0.28
Astore	LR s	0.03	0.05	0.06	0.00	0.02	0.04	0.08	0.05	0.01	0.04
Astore	LR p	0.02	0.05	0.01	0.87	0.23	0.01	0.00	0.11	0.76	0.09
Bunji	MK	0.01	0.00	0.03	0.82	0.02	0.58	0.01	0.73	0.07	0.42
Bunji	LR s	0.04	0.07	0.06	−0.01	0.04	0.01	0.06	0.01	−0.03	0.02
Bunji	LR p	0.00	0.00	0.01	0.81	0.04	0.38	0.01	0.73	0.13	0.29
Gilgit	MK	0.16	0.42	0.76	0.03	0.49	0.00	0.00	0.33	0.93	0.01
Gilgit	LR s	−0.01	0.02	0.01	−0.05	−0.02	0.05	0.09	0.06	0.00	0.07
Gilgit	LR p	0.41	0.39	0.62	0.02	0.41	0.00	0.00	0.07	0.85	0.00
(b) Station	Var.	Year st.	LT	Before	After	St.	Var.	Year st.	LT	Before	After
Astore	$T_{min\ JFM}$	2002	−4.4	−4.8	−3.7	Bunji	$T_{min\ OND}$	1997	5.1	4.9	5.5
Astore	T_{minAMJ}	1999	7.6	7.2	8.4	Bunji	T_{maxJFM}	1997	13.8	13.3	14.5
Astore	T_{maxY}	1998	15.7	15.3	16.2	Gilgit	D_{wY}	2001	39.3	33.6	53.4
Astore	T_{maxJFM}	2000	5.4	4.8	6.4	Gilgit	T_{minJAS}	1986	15.6	16.7	15.3
Bunji	T_{minY}	2003	10.9	10.7	11.7	Gilgit	T_{maxY}	1995	24.1	23.7	24.6
Bunji	T_{minJFM}	1997	3.5	3.1	4.1	Gilgit	T_{maxJFM}	1995	13.8	13	14.6
Bunji	T_{minAMJ}	2001	15.3	15	16.2	Gilgit	T_{maxOND}	1991	18.9	18.2	19.3
(c)	Y	JFM	AMJ	JAS	OND	–	Y	JFM	AMJ	JAS	OND
DT_G/T_{min}	0.21	0.25	0.35	−0.16	0.19	NAO/D_w	−0.32	−0.44	0.33	−0.33	−0.10
DT_G/T_{max}	0.55	0.41	0.24	0.11	0.33	NAO/T_{min}	0.00	−0.36	−0.26	0.05	0.12
NAO/P_m	−0.14	0.10	0.17	0.18	0.17	NAO/T_{max}	−0.21	−0.23	−0.22	0.06	−0.05

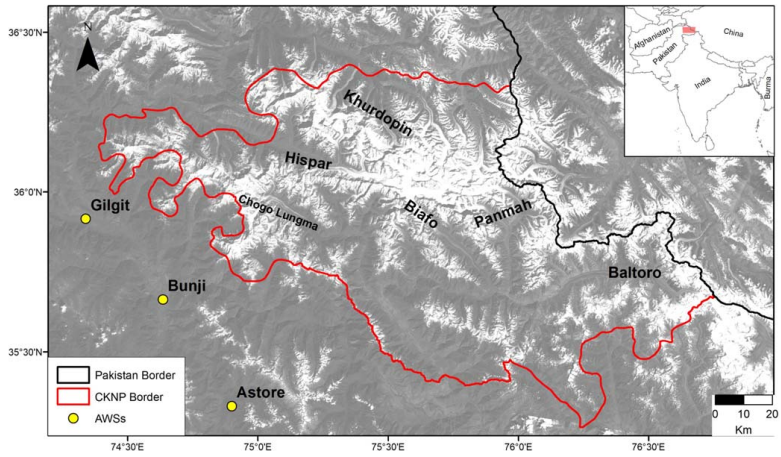

Fig. 1. Study area, the Central Karakoram National Park (CKNP) in northern Pakistan. AWSs (Automatic Weather Stations) considered in this study are highlighted in yellow.

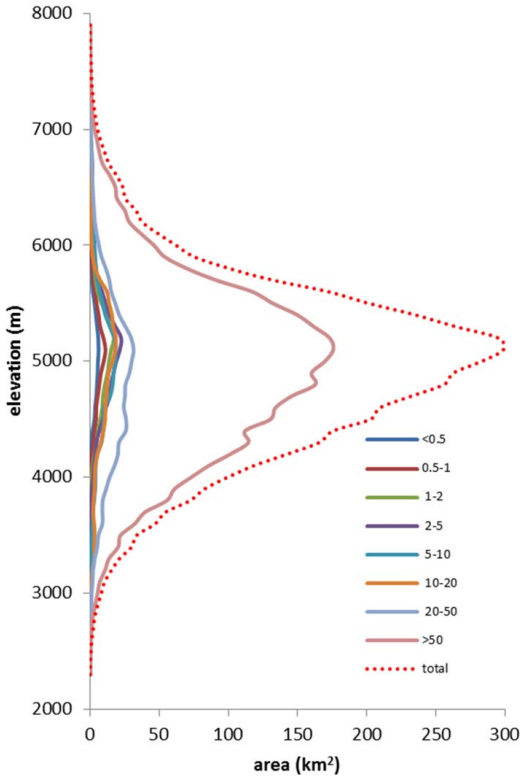

Fig. 2. Hypsography of glacier area distribution per area class by 100 m elevation bins (based on 2001).

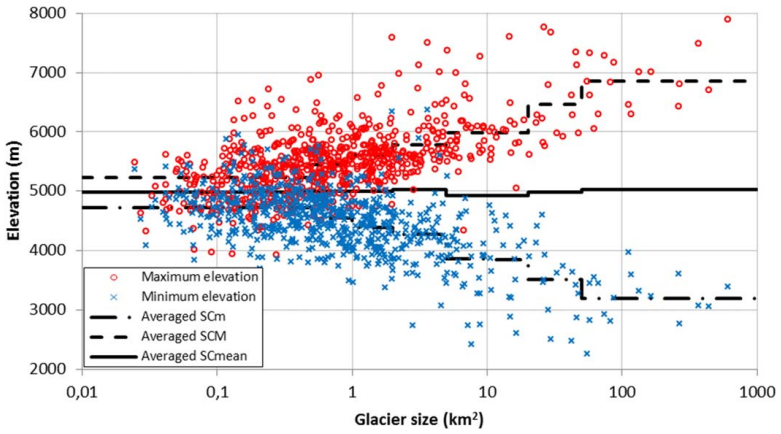

Fig. 3. Minimum and maximum elevation versus area size (2001). Values for discrete size classes are also given (SC = Size Class; m/M = minimum/Maximum). Notice the logarithmic scale for glacier size.

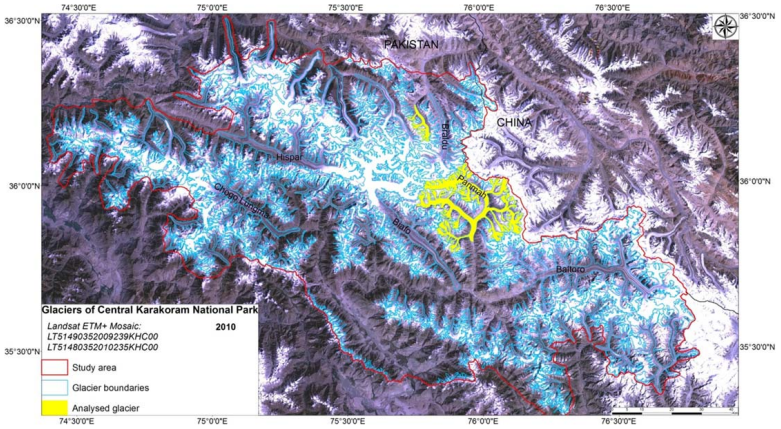

Fig. 4. 2010 CKNP glacier coverage, based on the Landsat 2010 (channels 321). The red line marks the study area boundary. Yellow outlines represent glaciers further analyzed in detail.

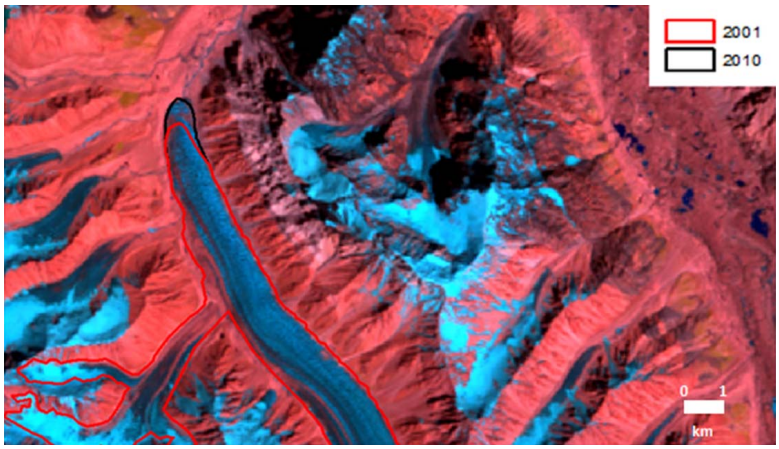

Fig. 5. Example of an advancing glacier terminus near Braldu glacier from 2001–2010. See Fig. 4 to see its location in the CKNP.

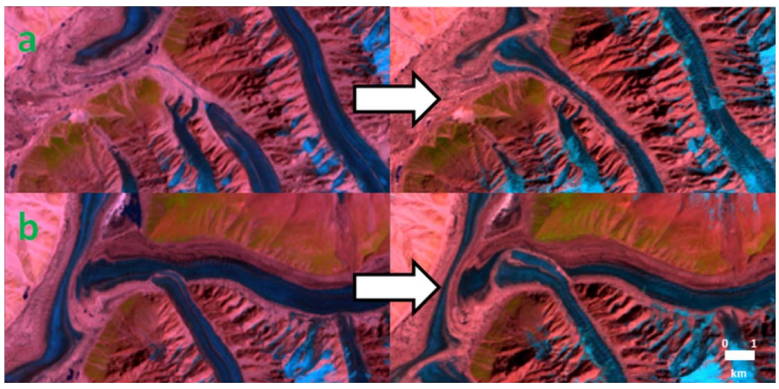

Fig. 6. (a, b) Comparison of Panmah's tributaries position in 2001 (left) and 2010 (right). See Fig. 4 for the location in the CKNP.

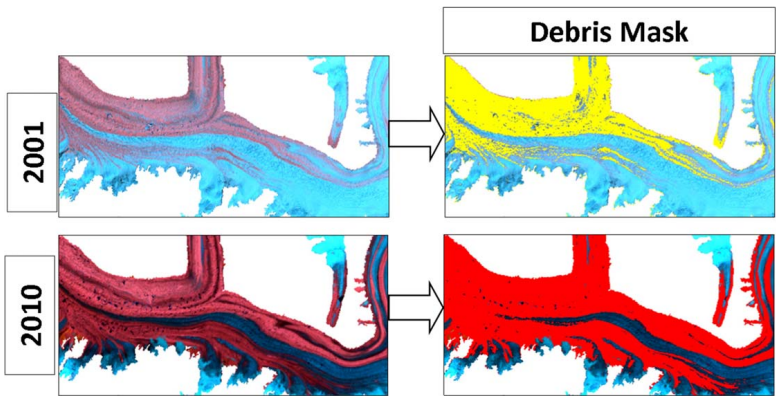

Fig. 7. Supraglacial debris coverage change for 2001 (upper figures) and for 2010 (lower figures).

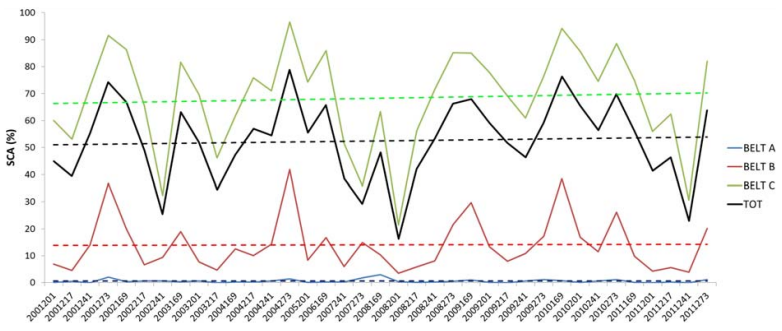

Fig. 8. Snow cover distribution (SCA) in three different altitudinal zones of the CKNP for the May–September windows of 2000/2011 period. Data Time Period is given in years and Julian days.

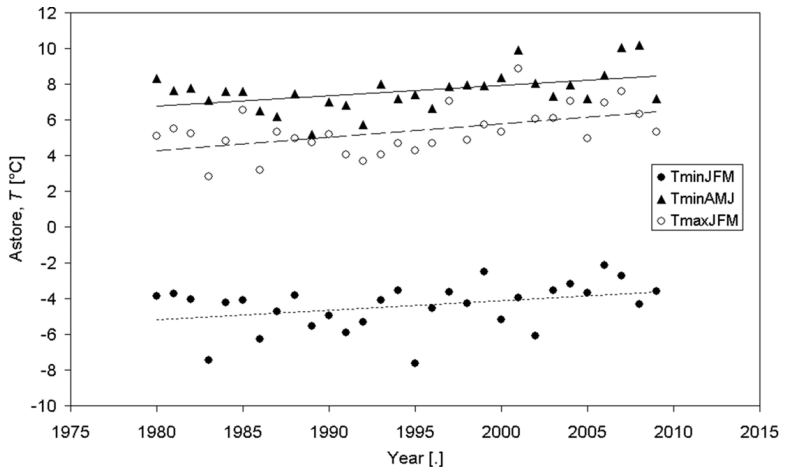

Fig. 9. Seasonal minimum air temperatures (winter: JFM, spring: AMJ) and winter maximum air temperatures for the station Astore, including their linear trends.

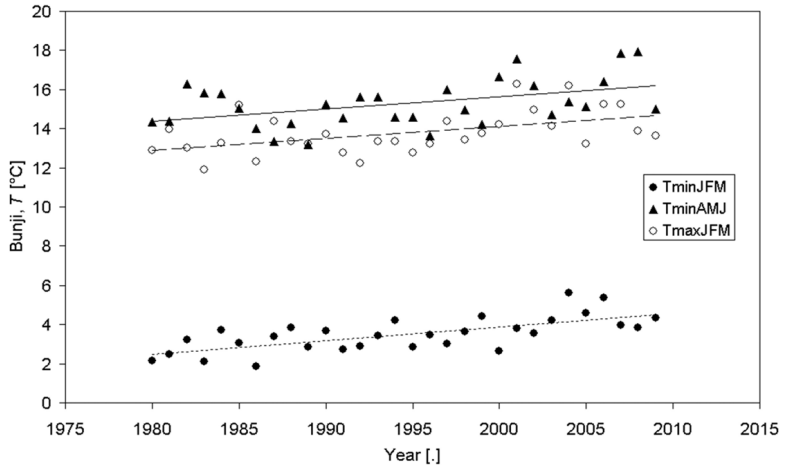

Fig. 10. Seasonal minimum air temperatures (winter: JFM, spring: AMJ) and winter maximum air temperatures for the station Bunji, including their linear trends.

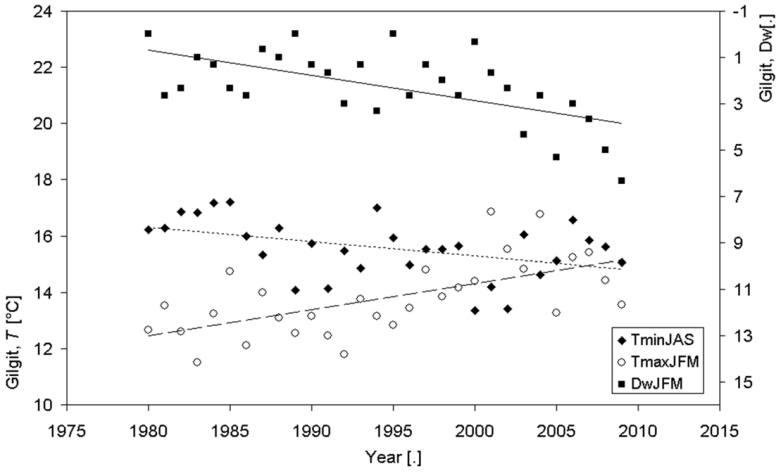

Fig. 11. Summer minimum air temperatures (JAS) and winter maximum air temperatures (JFM) for the station Gilgit, including their linear trends. In addition also the number of wet days D_w during winter is displayed.